



This is a repository copy of *Physical Mechanisms Responsible for the Water-Induced Degradation of PC61BM P3HT Photovoltaic Thin Films*.

White Rose Research Online URL for this paper:
<http://eprints.whiterose.ac.uk/93404/>

Version: Accepted Version

Article:

Parnell, A.J., Cadby, A.J., Dunbar, A.D.F. et al. (5 more authors) (2016) Physical Mechanisms Responsible for the Water-Induced Degradation of PC61BM P3HT Photovoltaic Thin Films. *Journal of Polymer Science Part B: Polymer Physics*, 54 (2). 141-146. ISSN 0887-6266

<https://doi.org/10.1002/polb.23902>

This is the peer reviewed version of the following article: Parnell, A. J., Cadby, A. J., Dunbar, A. D. F., Roberts, G. L., Plumridge, A., Dalglish, R. M., Skoda, M. W. A. and Jones, R. A. L. (2016), Physical mechanisms responsible for the water-induced degradation of PC61BM P3HT photovoltaic thin films. *J. Polym. Sci. B Polym. Phys.*, 54: 141–146, which has been published in final form at <http://dx.doi.org/10.1002/polb.23902>. This article may be used for non-commercial purposes in accordance with Wiley Terms and Conditions for Self-Archiving (<http://olabout.wiley.com/WileyCDA/Section/id-820227.html>)

Reuse

Unless indicated otherwise, fulltext items are protected by copyright with all rights reserved. The copyright exception in section 29 of the Copyright, Designs and Patents Act 1988 allows the making of a single copy solely for the purpose of non-commercial research or private study within the limits of fair dealing. The publisher or other rights-holder may allow further reproduction and re-use of this version - refer to the White Rose Research Online record for this item. Where records identify the publisher as the copyright holder, users can verify any specific terms of use on the publisher's website.

Takedown

If you consider content in White Rose Research Online to be in breach of UK law, please notify us by emailing eprints@whiterose.ac.uk including the URL of the record and the reason for the withdrawal request.



eprints@whiterose.ac.uk
<https://eprints.whiterose.ac.uk/>

Physical mechanisms responsible for the water induced degradation of PC₆₁BM P3HT photovoltaic thin films

Andrew J. Parnell^{1*}, Ashley J. Cadby¹, Alan D. F. Dunbar², George Roberts^{1#}, Alex Plumridge^{1†}, Robert M. Dalgliesh³, Maximillian W. A. Skoda³, and Richard A. L. Jones¹

¹Department of Physics and Astronomy, The University of Sheffield, S3 7RH, UK

²Department of Chemical and Biological Engineering, The University of Sheffield, Sir Robert Hadfield Building, Mappin St, Sheffield, S1 3JD, UK

³ISIS Pulsed Neutron and Muon Source, Science and Technology Facilities Council, Rutherford Appleton Laboratory, Harwell Science and Innovation Campus, Didcot OX11 0QX, UK

#Current address Engineering Department, Centre for Advanced Photonics and Electronics, University of Cambridge, 9 JJ Thomson Avenue, CB3 0FA

†Current address Department of Physics, 109 Clark Hall, Cornell University, Ithaca, New York, USA

Correspondence to: Andrew Parnell (E-mail: a.j.parnell@sheffield.ac.uk)

((Additional Supporting Information may be found in the online version of this article.))

ABSTRACT

We show that [6,6]-phenyl-C61-butyric acid methyl ester (PC₆₁BM) at the surface of thin film blends of poly(3-hexylthiophene) (P3HT):PC₆₁BM can be patterned by water. Using a series of heating and cooling steps water droplets condense onto the blend film surface. This is possible due to the liquid like, water swollen layer of PEDOT:PSS. Breath pattern water deformation and subsequent drying on the film surface results in isolated PC₆₁BM structures, showing that migration of PC₆₁BM takes place. This was confirmed by selective wavelength illumination to spatially map the photoluminescence from the P3HT and PC₆₁BM. Within a device redistribution of the surface PC₆₁BM into aggregates would be catastrophic, as it would dramatically alter device performance. We also postulate that repeated volume change of the PEDOT:PSS layer by water swelling may be in part responsible for the delamination failure mechanism in thin film solar cells devices.

This communication examines the effect of heating and cooling on the integrity of a well studied polymer solar cell blend system, that of P3HT:PC₆₁BM. Our device architecture also used the hole transport layer PEDOT:PSS below the solar cell layer. We have examined this system when exposed to heating and cooling cycles of the kind that may be experienced during

working operation out in the real world. In particular we examined the impact on the surface of this thin polymer film system. Our findings show that under humid conditions the swollen PEDT:PSS layer makes it possible for water droplets to condense on the blend film surface, evaporation of the water leaves behind microscale surface deformations. We also

observe that water evaporation drives deposition of the PC₆₁BM to the base of the breath pattern deformation, making it no longer uniformly distributed across the blend film surface removing the nanoscale morphology^[1] and contact area needed for high efficiency devices.

Polymer-based electronics have attracted huge interest due to their low processing costs and large area coating potential. They have wide applicability: as light emitting diodes for displays, field effect transistors, organic photovoltaics (OPV's) and also low power lighting. Thin film polymer and hybrid OPV solar cells have advanced technologically very rapidly - they are now close to the point of being considered industrially viable on a large scale^[2,3]. This has been made possible by the sheer intensity of the research into numerous material and processing aspects. These include; combinatorial studies of blend ratios, structure evolution upon thermal and also solvent annealing, polymer synthesis design and optimization to maximize light absorption of the solar spectrum^[4,5]. What has not been studied to the same extent is their degradation and stability, ultimately it could be argued that this is what will determine the long term viability and roll out of OPV technology in the wider mass market^[6].

PC₆₁BM has proved an important material for polymer electronics and particularly OPVs. Principally PC₆₁BM is an excellent electron acceptor that when blended with a suitable conjugated polymer is able to produce free charges with high efficiency. The use of PC₆₁BM in bulk heterojunction blend devices removed the problem of interface bound charge transfer states, long associated with polymer-polymer based devices and one of the major limitations

in producing high efficiency OPV devices^[7] in all polymer systems which currently stand at around 4-5% efficiency^[8,9].

The P3HT:PC₆₁BM thin film sample used in this study has a surface enrichment of fullerene prior to any heating treatment (i.e. as spin cast) determined using neutron reflectivity (see SI 1)^{[10] [11]}. Using the known values for the neutron scattering length densities it is possible to deduce that this thin 10 nm surface layer is ~ 50 % fullerene by volume. Figure 1a shows an optical microscope image of the surface of a PC₆₁BM P3HT blend film that has been subjected to a number of heating and cooling cycles up to 65 °C and down to -20 °C and finally up to 180 °C for 60 min. What is clear is that these film surfaces look on first sight very different to the long time thermally annealed films seen frequently in the literature. Where long time annealing at temperatures above ~150 °C gives rise to large PC₆₁BM crystallites on the film surface^[12,13]. The appearance of the circular features is somewhat surprising given the fact that the surface of the blend films is a spin coated film and nominally very smooth ~ 1 nm surface roughness^[14]. We attribute these strong surface features to breath pattern structuring of the thin film surface. Breath pattern figures are formed when water droplets condense onto a surface, by regulating the flow rate of humid air the pattern size and degree of ordering can be controlled^[15] and this has been extensively studied for solvent molten polymer layers. The water droplets have sufficient mass to cause depressions on the film surface, the structure of these features remain after the droplets evaporate. The initial study first reporting them used solvent cast films; some solvent was present when the surface droplets formed, i.e. they were in a molten state. Breath patterns are essentially out of plane

deformations due to the stress of the water droplets on the film surface. Subsequent work has seen similar structures in water exposed pure polymer films^[16].

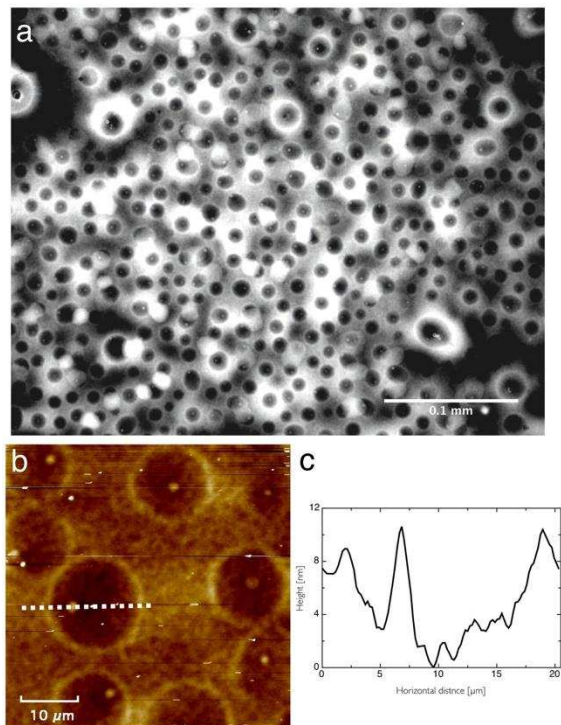


FIGURE 1. Crater features on the surface of the PC₆₁BM:P3HT thin film blend. **a** an optical microscopy image showing the occurrence of the craters over the surface. **b** a scanning probe image over a smaller region showing the depression in the thin film along with the point like deposit inside every crater. **c** a line scan across the dashed line in **b** showing the rim of the crater, its depth and the point like nanostructure.

Figure 1a shows an optical micrograph and 1b shows a higher resolution scanning probe microscopy image of a smaller region of the OPV blend film surface, where the breath pattern features can clearly be observed, the crater or depression has a lower height than the surrounding film, the breath pattern feature also has a spherical crater rim. The line section

in Fig. 1c shows the profile of the crater. Interestingly there is a nanoscale aggregate located within each crater, this is observed in all the spherical craters.

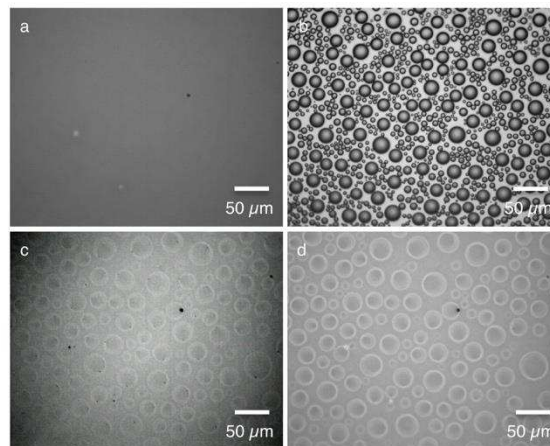


FIGURE 2. Optical microscopy images of a PC₆₁BM:P3HT thin film undergoing a series of heating and cooling cycles. **a** room temperature, **b** cooled, at this point the water condenses, **c** heated to 65 °C, **d** heated further to 180 °C.

In situ optical microscopy was carried out to confirm that the mechanism responsible for these surface features is breath pattern induced stress deformation of the film. Figure 2 shows a series of optical images for a thin PC₆₁BM:P3HT blend film on PEDOT:PSS film that received the same thermal treatment of being heated up to 65 °C and then cooled down to -20 °C, figure 2b clearly shows the surface of the film populated with micron scale water droplets caused by condensation from the air. As the temperature is raised in Fig 2c the droplets evaporate and a remnant cratered depression feature is left on the surface of the thin film. Subsequent heating to 180 °C shows that these surface features remain.

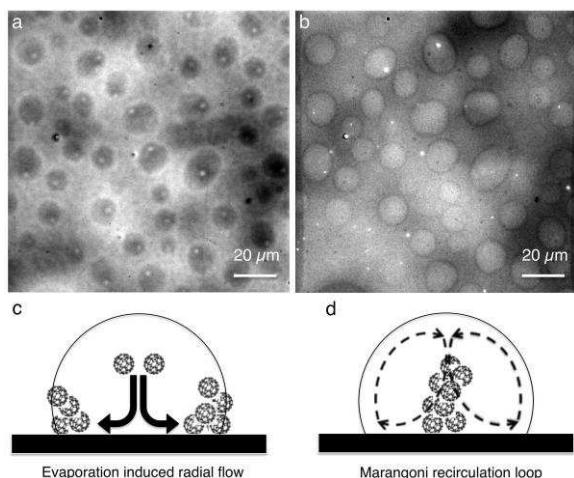


FIGURE 3. Photoluminescence maps for a thin P3HT:PC₆₁BM blend film that has been heated and cooled repeatedly (undergoing the same heating cooling cycle outlined in the sample preparation). **a** when illuminated with 405 nm light which is strongly absorbed by PC₆₁BM, **b** when illuminated with 473 nm which is strongly absorbed by P3HT, **c** and **d** are the possible mechanisms driving the deposition and movement of the PC₆₁BM.

To further understand the composition of the central aggregate structures that remain in the water induced deformation craters, we have performed photoluminescence (PL) mapping of the sample surface. By probing the OPV blend thin film using light with wavelengths of 405 nm for the PC₆₁BM^[17] and 473 nm for the P3HT^[18] we are able to differentiate between the two blend components and so spatially map the distribution of PC₆₁BM and P3HT at the film surface. This technique shows that PC₆₁BM is located at the outer droplet rim and also the aggregate located within the perimeter of the droplet is predominantly made of PC₆₁BM. Clearly there must be some mechanism, which can readily deform the surface structure and redistribute the PC₆₁BM on the surface. The key to understanding the mechanism behind these nanoscale surface features is that on cooling

the sample water droplets condense on the film surface, whilst the underlying PEDOT:PSS layer is swollen with water and therefore deformable. As a result, when the water droplet imparts a deformation stress on the film, its surface is restructured. To understand this further we performed a further experiment to unambiguously quantify the water content in spin coated PEDOT:PSS thin films. The material PEDOT:PSS is widely used as a hole transport layer between the electrode (commonly Indium Tin Oxide, ITO) and the active layer. The NR data shown in Fig. 4 is for a thin film of PEDOT:PSS only, spin coated onto silicon, making the modeling more straightforward. It shows a dramatic change in film thickness of over 20% (7.1 nm), with an initial thickness of 34.8 nm and a scattering length density (SLD) $1.455 \times 10^{-6} \text{ \AA}^{-2}$ in ambient air, and after annealing at 180 °C under dry nitrogen the thickness this had reduced to 28 nm and an SLD of $1.923 \times 10^{-6} \text{ \AA}^{-2}$. Using the SLD value for the annealed dry film we can calculate that the ambient film has ~ 19% by volume of water, and so agrees with the change in thickness between the ambient and thermally annealed thin film.

For the case of the P3HT:PC₆₁BM PEDOT:PSS bilayer system, upon increasing the temperature, the water droplets on the active layer surface slowly evaporate and their volume reduces accordingly, whilst maintaining a circular shape. There are two drying pattern structures that clearly be seen clearly in the SFM image (Fig 1 b). These are coffee ring structures at the perimeter of the droplet and a more central aggregate structure. Over time the water evaporates and the concentration of the nano-particulate suspension of PC₆₁BM increases to become substantially more concentrated. At the end of the evaporation process, the droplet shape and concentration

reach a point of instability. At this point the water drop finally becomes unstable and the PC₆₁BM molecules are deposited in a small restricted area to form the PC₆₁BM aggregate deposit seen within each depression^[19]. The competition between pinning at the initial droplet contact line (Fig. 3c) and the inward flux of water is responsible for driving the PC₆₁BM within the perimeter of the water droplet deformation (fig. 3d)^[20]. This inward water flux is possibly due to a Marangoni recirculation loop depositing the PC₆₁BM in a central aggregate structure^[21].

It is also assumed that in a similar manner during the formation and growth of the condensed water droplets on the surface the PC₆₁BM is driven outwards towards the edge and subsequently deposited at the rim of the crater like depressions.

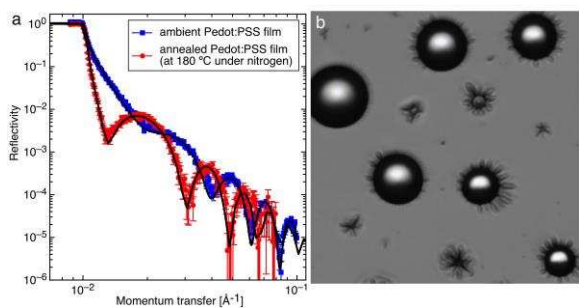


FIGURE 4. a neutron reflectivity data for a spin coated Pedot:PSS thin film on silicon, showing the change in reflectivity before and after thermal annealing. b optical microscopy showing capillary wrinkling of the OPV blend film surface by the water droplets.

Wrinkling of the OPV blend on PEDOT:PSS films at the edge of each droplet can be seen in the graphical figure 4 b. The presence of these wrinkles in the films further evidences the mechanisms proposed, and they can be used to probe the viscoelastic properties of ultrathin films. They are attributed to the deformation

stress caused by the formation of the condensed water droplets on top of the film acting on the P3HT:PC₆₁BM film, which is able to partially deform into the molten water swollen PEDOT:PSS layer below. These out of plane instabilities have been observed previously for poly(styrene) thin films floated on a water substrate surface with water droplets on the top surface.^[22] If water is taken into the PEDOT:PSS layer from the edges as has been shown^[23] it will swell and likely cause similar out of plane deformations in the other layers (OPV layer and the metal cathode layer). This may be the origin of the bubble like surface features often seen in thin film polymer electronics where PEDOT:PSS is used as a hole transport layer^{[24] [25]}. Conventional OPV device processing is to heat treat the PEDOT:PSS prior to deposition of any subsequent layers and so any ambient moisture will be initially absent but an uptake of moisture during device operation will cause a swelling of at least 20 % for this layer. This will likely give rise to out of plane deformations.

In conclusion we have observed some behavior not seen before in thin film PC₆₁BM OPV blend films, in that they can be patterned by water. As such, water ingress to thin films can move PC₆₁BM and cause aggregation structures that in a device would remove a large majority of the contact area, causing a huge reduction in device performance. The deformation features seen on the surface are due to the liquid like PEDOT:PSS layer that is water swollen; repeated swelling deswelling cycles of this layer are liable to cause buckling and stress between the active layer and the metal cathode interface, again reducing the effectiveness of any OPV device. The incorporation of PEDOT:PSS and PC₆₁BM as hole and electron transport layers in devices such as hybrid OPV and Perovskite based devices is also routine, so our results have important implications for the field of

multilayer functional materials that use these materials as layers in any device or any water soluble hole transport layer^[26].

ACKNOWLEDGEMENTS

We acknowledge ISIS spallation neutron source (UK) for allocation of beamtime on the ISIS instruments SURF and OFFSPEC. AJP is grateful to Professor J. Patrick A. Fairclough for helpful discussions during the preparation of this manuscript.

EXPERIMENTAL

Sample preparation

P3HT was obtained from Merck (Lisicon SP001 Batch EF 430302 M_w 54.3k M_n 23.6 k). The PC₆₁BM was obtained from Solenne BV. Solutions of P3HT and PC₆₁BM were prepared separately in filtered chlorobenzene at a concentration 25 mg per mL. The two solutions were then mixed in a proportion of 1:0.7 PC₆₁BM:P3HT. The solutions was spin cast onto PEDOT:PSS (Clevios AI4083) coated single crystal silicon wafers (Prolog Semicor) having a diameter of 50 mm and 5 mm thickness (necessary for the NR measurements) at a spin speed of 2000 rpm for 30 s.

The sample was analyzed by neutron reflectivity at various times during several relatively short thermal cycles followed by a longer *in situ* thermal anneal. The thermal cycles were performed using a Linkam hot stage in air, initially ramping the sample to 50 °C followed by immediate cooling. Subsequent cycles included a ramp and hold at 50 °C for 1 minute, 5 minutes at 65 °C and finally 90 minutes at 180 °C. In the cooling part of the each cycle the sample was cooled to -20 °C.

Sample Characterization

Thin films were characterized using a J. A. Woolam M2000V spectroscopic ellipsometer (370 nm-1000 nm) with the data fitted using a

Cauchy model. Although only data in the wavelength range 700 nm - 1000 nm (non-optically absorbing region) was used to determine the film thickness. Films were also characterized using a scanning force microscope (Veeco Dimension 3100) operating in tapping mode. The scanning force microscopy (SFM) tips were standard Olympus tapping tips with a resonance around ~ 280 kHz. The SFM images were analysed using the freely available analysis program ImageSXM to calculate the root mean square roughness.

Neutron reflectivity (NR) measurements were performed on the SURF and OFFSPEC reflectometers at the ISIS spallation neutron source (Rutherford Appleton Laboratory, UK). The SURF reflectometer has a range of neutron wavelengths (0.5 Å – 6.55 Å) and uses a time-of-flight detection system. Three incident angles were used to obtain the sample reflectivity as a function of the momentum transfer perpendicular to the sample plane, q_z . The NR data was analyzed using previously developed routines^[14,27]. Where a stack of thin recursive layers is used in the model in which each layer is characterized by a thickness, roughness and scattering length density (after the scheme of Névot and Croce)^[28]. Experimental data were then fitted using a least-squares fit in which a series of starting values were trialed in order to find a global minimum. From the final fit values of the scattering length density we could calculate the relative volume fractions of polymer (blend) and water in each layer. These water-condensed samples are expected to scatter off specularly due to the presence of the water condensed surface features (see Fig. 1), however the length scales are too large (10 μm – 20 μm) for us to study. Details of the OFFSPEC instruments can be found in the following publications^[29,30].

Heating protocol for chamber NR measurements

The PEDOT:PSS thin film sample on a silicon wafer was placed inside the sample chamber and aligned with respect to the neutron beam. It was first of all measured in air. Subsequently the chamber was evacuated followed by a number of purge cycles with dry Nitrogen gas. The sample was then thermally annealed at 180 °C for 60 minutes with a flow of Nitrogen gas. The chamber was cooled to room temperature and the reflectivity was measured again.

Photoluminescence measurements

A bespoke epifluorescence optical system was used to measure the Photoluminescence (PL). Separate LED light sources were used with wavelengths of 405 nm light for PC₆₁BM^[17] and 473 nm for the P3HT^[18]. The microscope system uses an objective with 63 times magnification and 1.4 numerical aperture (Zeiss). Band pass filters were used to separate P3HT emission from that of PC₆₁BM. Images were collected using a cooled Princeton EMCCD.

REFERENCES AND NOTES

- [1] A. J. Parnell, A. J. Cadby, O. O. Mykhaylyk, A. D. F. Dunbar, P. E. Hopkinson, A. M. Donald, R. A. L. Jones, *Macromolecules* **2011**, *44*, 6503.
- [2] M. Graetzel, R. A. J. Janssen, D. B. Mitzi, E. H. Sargent, *Nature* **2012**, *488*, 304.
- [3] R. R. Søndergaard, M. Hösel, F. C. Krebs, *Journal of Polymer Science Part B: Polymer Physics* **2012**, *51*, 16.
- [4] W. Ma, C. Yang, X. Gong, K. Lee, A. J. Heeger, *Adv. Funct. Mater.* **2005**, *15*, 1617.
- [5] S. H. Park, A. Roy, S. Beaupré, S. Cho, N. Coates, J. S. Moon, D. Moses, M. Leclerc, K. Lee, A. J. Heeger, *Nature Photon* **2009**, *3*, 297.
- [6] R. Gaudiana, *Journal of Polymer Science Part B: Polymer Physics* **2012**, *50*, 1014.
- [7] R. H. Friend, M. Phillips, A. Rao, M. W. B. Wilson, Z. Li, C. R. McNeill, *Faraday Discuss.* **2012**, *155*, 339.
- [8] T. Earmme, Y.-J. Hwang, S. Subramaniyan, S. A. Jenekhe, *Advanced Materials* **2014**, *26*, 6080.
- [9] Y. Zhou, T. Kurosawa, W. Ma, Y. Guo, L. Fang, K. Vandewal, Y. Diao, C. Wang, Q. Yan, J. Reinspach, J. Mei, A. L. Appleton, G. I. Koleilat, Y. Gao, S. C. B. Mannsfeld, A. Salleo, H. Ade, D. Zhao, Z. Bao, *Adv. Mater. Weinheim* **2014**, *26*, 3767.
- [10] R. A. L. Jones, E. J. Kramer, *Polymer* **1993**, *34*, 115.
- [11] P. A. Staniec, A. J. Parnell, A. Dunbar, H. Yi, A. J. Pearson, T. Wang, P. E. Hopkinson, C. Kinane, R. M. Dalgliesh, A. M. Donald, A. J. Ryan, A. Iraqi, R. A. L. Jones, D. G. Lidzey, *Advanced Energy Materials* **2011**, *1*, 499.
- [12] A. J. Parnell, R. M. Dalgliesh, R. A. L. Jones, *Applied Physics Letters* **2013**, *102*, 073111.
- [13] M. Campoy-Quiles, T. Ferenczi, T. Agostinelli, P. G. Etchegoin, Y. Kim, T. D. Anthopoulos, P. N. Stavrinou, D. D. C. Bradley, J. Nelson, *Nature Materials* **2008**, *7*, 158.
- [14] A. J. Parnell, A. D. F. Dunbar, A. J. Pearson, P. A. Staniec, A. J. C. Dennison, H. Hamamatsu, M. W. A. Skoda, D. G. Lidzey, R. A. L. Jones, *Advanced Materials* **2010**, *22*, 2444.
- [15] M. Srinivasarao, D. Collings, A. Philips, S. Patel, *Science* **2001**, *292*, 79.
- [16] J. S. Sharp, R. A. L. Jones, *Advanced Materials* **2002**, *14*, 799.
- [17] S. Cook, H. Ohkita, Y. Kim, J. J. Benson-Smith, D. D. C. Bradley, J. R. Durrant, *Chemical Physics Letters* **2007**, *445*, 276.
- [18] A. R. S. Kandada, G. Grancini, A. Petrozza, S. Perissinotto, D. Fazzi, S. S. K. Raavi, G. Lanzani, *Sci. Rep.* **2013**, *3*, 1.
- [19] F. De Angelis, F. Gentile, F. Mecerini, G. Das, M. Moretti, P. Candeloro, M. L. Coluccio, G. Cojoc, A. Accardo, C.

- Liberale, R. P. Zaccaria, G. Perozziello, L. Tirinato, A. Toma, G. Cuda, R. Cingolani, E. Di Fabrizio, *Nature Photon* **2011**, *5*, 683.
- [20] B. J. Fischer, *Langmuir* **2002**, *18*, 60.
- [21] R. Bhardwaj, X. Fang, P. Somasundaran, D. Attinger, *Langmuir* **2010**, *26*, 7833.
- [22] J. Huang, M. Juskiewicz, W. H. de Jeu, E. Cerda, T. Emrick, N. Menon, T. P. Russell, *Science* **2007**, *317*, 650.
- [23] T. S. Glen, N. W. Scarratt, H. Yi, A. Iraqi, T. Wang, J. Kingsley, A. R. Buckley, D. G. Lidzey, A. M. Donald, *Solar Energy Materials and Solar Cells* **2015**, *140*, 25.
- [24] V. N. Savvate'ev, A. V. Yakimov, D. Davidov, R. M. Pogreb, R. Neumann, Y. Avny, *Applied Physics Letters* **1997**, *71*, 3344.
- [25] R. Czerw, D. L. Carroll, H. S. Woo, Y. B. Kim, J. W. Park, *J. Appl. Phys.* **2004**, *96*, 641.
- [26] J. You, Z. Hong, Y. M. Yang, Q. Chen, M. Cai, T.-B. Song, C.-C. Chen, S. Lu, Y. Liu, H. Zhou, Y. Yang, *ACS Nano* **2014**, *8*, 1674.
- [27] J. W. Kingsley, P. P. Marchisio, H. Yi, A. Iraqi, C. J. Kinane, S. Langridge, R. L. Thompson, A. J. Cadby, A. J. Pearson, D. G. Lidzey, R. A. L. Jones, A. J. Parnell, *Sci. Rep.* **2014**, *4*, 5286.
- [28] L. Nevot, P. Croce, *Rev. Phys. Appl. (Paris)* **1980**, *15*, 761.
- [29] R. M. Dalgliesh, S. Langridge, J. Plomp, V. O. de Haan, A. A. van Well, *Physica B: Condensed Matter* **2011**, *406*, 2346.
- [30] A. J. Parnell, A. Hobson, R. M. Dalgliesh, R. A. L. Jones, A. D. F. Dunbar, *Journal of visualized experiments : JoVE* **2014**, e51129.

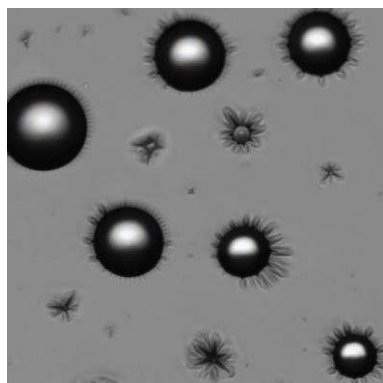
GRAPHICAL ABSTRACT

Andrew J. Parnell, Ashley J. Cadby, Alan D. F. Dunbar, George Roberts, Alex Plumridge, Robert M. Dalgliesh, Maximillian W. A. Skoda, and Richard A. L. Jones.

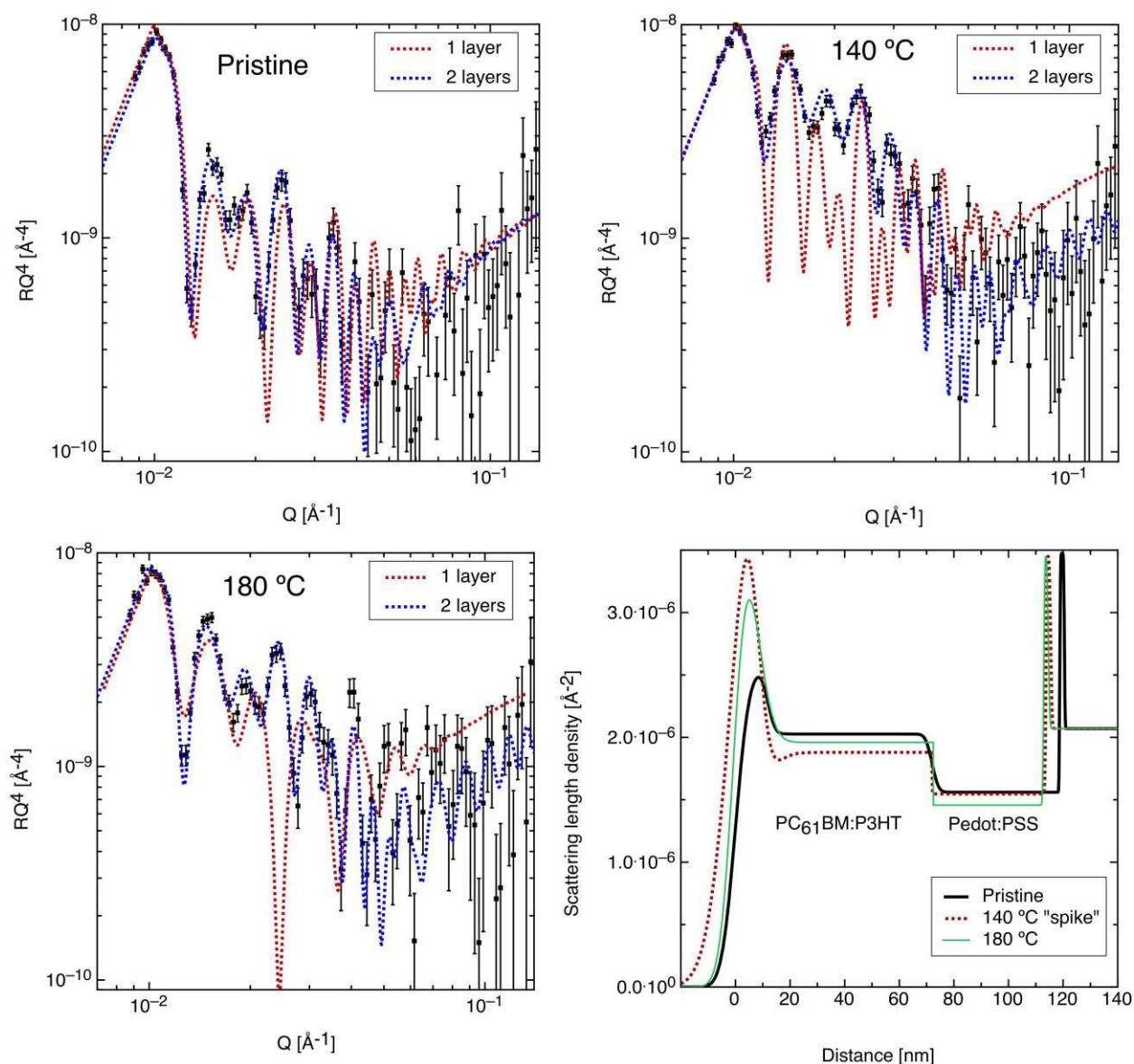
Physical mechanisms responsible for the water induced degradation of PC₆₁BM P3HT photovoltaic thin films

The water induced degradation mechanisms in polymer and hybrid polymer solar cells are explored by simulating the heating and cooling cycles that may be experienced during their operation. The surface distribution of PC₆₁BM can be dramatically altered from a planar uniform distribution by the presence of water, as breath pattern type structures are readily formed on the surface. These surface indentations are made possible by the liquid-like and swollen nature of the PEDOT:PSS layer.

GRAPHICAL ABSTRACT FIGURE



Supporting information



SI Figure 1. Neutron reflectivity for the sample studied in detail in these measurements prior to any thermal treatment (pristine), after the temperature jump to 140 °C followed by a temperature quench and finally prolonged heating at 180 °C for 90 minutes. The scattering length density of PC₆₁BM is much larger than that of P3HT and therefore shows a surface enriched in PC₆₁BM, when compared to the bulk of the blend film. The three fitted reflectivity datasets and the profiles based on the chi squared per point fitting approach to modeling the data can be seen in the bottom right hand panel

To enable comparison of the quality of the fits we have included the chi squared per point values for the three fitted datasets for the different temperature treatments of the OPV blend layer.

Pristine 1 layer 2.34 chi squared per point

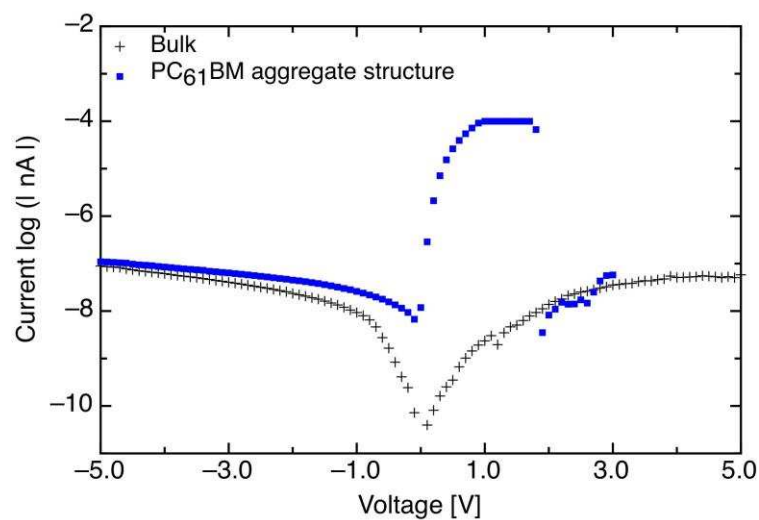
Pristine 2 layers 6.0 chi squared per point

140°C 1 layer 24.42 chi squared per point

140°C 2 layer 2.838 chi squared per point

180°C 1 layer 12.84 chi squared per point

180°C 2 layers 2.534 chi squared per point



SI Figure 2. Spatial current voltage (I-V) Electrical characterization of the bulk of the P3HT:PC₆₁BM film and the PC₆₁BM aggregate region.

The figure SI 2 shows that spatially the I-V characteristics of the film have been altered due to the water droplet deformation and restructuring.